Spin Density in the Heterodinuclear Compound Cu(salen)Ni(hfa)$_2$: A Polarized Neutron Diffraction Study

Béatrice Gillon,*,† Christian Cavata,† Peter Schweiss,† Yves Journaux,‡ Olivier Kahn,*,‡ and Daniel Schneider‡

Contribution from the Laboratoire Léon Brillouin, Laboratoire Commun CEA—CNRS, CEN Saclay, 91191 Gif sur Yvette, France, and Laboratoire de Chimie Inorganique, URA 420, Université de Paris-Sud, 91405 Orsay, France. *Received January 6, 1989*

Abstract: The spatial spin distribution for the title compound in its doublet ground state has been determined from polarized neutron diffraction (PND) at 2 K and within an applied magnetic field of 5×10^4 G. Two sets of data have been collected, providing 76 and 212 independent reflections, respectively, with $|F| > 3\sigma$. To obtain the spin density, a multipole model has been used, consisting of a superposition of atomic densities, developed on the basis of multipolar functions, product of a radial function of Slater type and a real spherical harmonics. The spin density map shows a strong positive zone in the nickel surroundings and a weak negative zone in the copper surroundings. The atomic spin populations were as follows: −0.25 (1) μ_B for the copper atom, 1.26 (1) μ_B for the nickel atom, an upper limit of 0.02 μ_B for the two bridging oxygen atoms, and a total of 0.14 (4) μ_B for the four peripheral oxygen atoms and of −0.02 μ_B for the two peripheral nitrogen atoms. The almost negligible spin population on the bridging oxygen atoms has been attributed to a compensation between a positive contribution coming from the nickel(II) ion and a negative contribution coming from the copper(II) ion, characterizing the antiferromagnetic nature of the Cu(II)–Ni(II) interaction. A semiempirical interpretation of the PND data has been proposed. The wave functions associated with the doublet ground state, of the Heitler–London type, were constructed by using the three magnetic orbitals as the basis set. Each of these magnetic orbitals has been calculated in the extended Hückel approximation by contracting the atomic orbitals of the metal ion on which it is not centered. The atomic spin populations calculated according to this approach not only are in fairly good agreement with those deduced from the PND data but also have led to a rather simple and heuristic picture of the exchange interaction in Cu(salen)Ni(hfa)$_2$. In addition to the spatial spin distribution study, the molecular structure of Cu(salen)Ni(hfa)$_2$ has been redetermined at 19.6 K by unpolarized neutron diffraction. The compound crystallizes in the monoclinic system, space group $P2_1/n$, $a = 9.16$ (5) Å, $b = 21.47$ (2) Å, $c = 14.70$ (3) Å, $\beta = 93.9$ (4)°, and $Z = 4$. The intramolecular Cu···Ni separation is rather short, 2.906 (5) Å, owing to a significant bending of the CuO_2Ni bridging network along the direction joining the two phenolic oxygen atoms.

A tremendous amount of work have been devoted to the understanding of the exchange interaction phenomenon in polymetallic molecular compounds.[1] It is definitely not possible to summarize, even briefly, all the studies dealing with this subject. It seems to us worthwhile, however, to point out the main advances that have emerged in the last 10 years or so: (i) The first qualitative model that has been proving to be successful is that of the active electrons.[2] This model directly arises from the pioneering work of Anderson.[3] It explictly takes into account the only unpaired electrons of the metal centers and the magnetic orbitals they occupy. Two variants of this model have been developed, the former with orthogonalized magnetic orbitals,[4] the latter with natural magnetic orbitals.[2] A good example of the possibilities of this model is provided by the interpretation of the role of the CuOCu bridging angle in hydroxo-bridged copper(II) dimers;[4-6] (ii) The importance of the relative symmetries of the interacting magnetic orbitals has been demonstrated in a clearcut fashion by comparing the magnetic properties of the two related compounds $Cu_2(fsa)_2en{\cdot}CH_3OH$ and $CuVO(fsa)_2en{\cdot}CH_3OH$, with $H_2(fsa)_2en$ = *N*,*N*′-(2-hydroxy-3-carboxybenzilidene)-1,2-diaminoethane. In the former compound, the two magnetic orbitals have the same symmetry; they do overlap and the spin–singlet is the ground state. In the latter compound, the two magnetic orbitals are strictly orthogonal and the spin–triplet is the ground state.[7] More generally, new exchange pathways may be obtained in heteropolymetallic systems and the studies dealing with compounds of that kind have played quite an important role in molecular magnetism;[8] (iii) In 1981, the first all valence electron ab initio calculation concerning a magnetically coupled compound appeared.[9] This calculation deals with copper(II) acetate and shows that several additional terms beside those considered in the active electron model may contribute significantly to the relative energies of the low-lying states. In the perturbational approach used for this calculation, these terms are defined as the double-spin polarization, the metal → ligand and ligand → metal charge transfers, the kinetic + polarization, etc. This approach has been extended to other copper(II) dinuclear compounds[10-15] as well as to the $CuVO(fsa)_2en{\cdot}CH_3OH$ compound mentioned above.[16] Other recent calculations are based on the broken symmetry formalism within the Xα scheme;[17-21] (iv) Finally, owing again

† Laboratoire Léon Brillouin.
‡ Laboratoire de Chimie Inorganique.

(1) See, for instance: Willett, R. D.; Gatteschi; D.; Kahn, O. *NATO ASI Series Ser. C* **1985**, *140*.
(2) Kahn, O. in ref 1, p 37, and references therein.
(3) Anderson P. W. *Solid State Phys.* **1963**, *14*, 99; In *Magnetism*; Rado, G. T., Suhl, H. Eds.; Academic Press: New York, 1963; Vol. 1, p 25.
(4) Hay, P. J.; Thibeault, J. C.; Hoffmann, R. *J. Am. Chem. Soc.* **1975**, *97*, 4884.
(5) Crawford, W. H.; Richardson, H. W.; Wasson, J. R.; Hodgson, D. J.; Hatfield, W. E. *Inorg. Chem.* **1976**, *15*, 2107.
(6) Charlot, M. F.; Jeannin, S.; Jeannin, Y.; Kahn, O.; Lucrece-Abaul, J.; Martin-Frere, J. *Inorg. Chem.* **1979**, *18*, 1675.
(7) Kahn, O.; Galy, J.; Journaux, Y.; Jaud, J.; Morgenstern-Badarau, I. *J. Am. Chem. Soc.* **1982**, *104*, 2165.
(8) Kahn, O. *Struct. Bonding (Berlin)* **1987**, *68*, 89, and references therein.
(9) De Loth, P.; Cassoux, P.; Daudey, J. P.; Malrieu, J. P. *J. Am. Chem. Soc.* **1981**, *103*, 4007.
(10) Daudey, J. P.; De Loth, P.; Malrieu, J. P. in ref 1, p 87.
(11) De Loth, P.; Daudey, J. P.; Astheimer, H.; Walz, L.; Haase, W. *J. Chem. Phys.* **1985**, *82*, 5048.
(12) Charlot, M. F.; Verdaguer, M.; Journaux, Y.; De Loth, P.; Daudey, J. P. *Inorg. Chem.* **1984**, *23*, 3802.
(13) Nepveu, F.; Haase, W.; Astheimer, H. *J. Chem. Soc., Faraday Trans. 2* **1986**, *82*, 551.
(14) Astheimer, H.; Haase, W. *J. Chem. Phys.* **1986**, *85*, 1427.
(15) Gehring, S.; Astheimer, H.; Haase, W. *J. Chem. Soc., Faraday Trans. 2* **1987**, *83*, 347.
(16) De Loth, P.; Karafiloglou, P.; Daudey, J. P.; Kahn, O. *J. Am. Chem. Soc.* **1988**, *110*, 5676.
(17) Ginsberg, A. P. *J. Am. Chem. Soc.* **1980**, *102*, 111.
(18) Bencini, A.; Gatteschi, D. *J. Am. Chem. Soc.* **1986**, *108*, 5763.
(19) Noodlman, L.; Baerends, E. J. *J. Am. Chem. Soc.* **1984**, *106*, 2316.
(20) Noodleman, L.; Norman, J. G., Jr.; Osborne, J.; Aizman, A.; Case, D. A. *J. Am. Chem. Soc.* **1985**, *107*, 3418, and references therein.

0002-7863/89/1511-7124$01.50/0

to the investigations dealing with heteropolymetallic systems, the relations between local and molecular **g**, zero-field splitting **D**, and hyperfine structure **A** tensors have been tested and their range of validity specified.[8,22,23] These relations are based on the assumption that the molecular functions can be constructed as products of local functions, which corresponds to the Heitler–London approach for weakly coupled systems.

So far, the kinds of information available for a given polymetallic system were the relative energies of the low-lying states as deduced from magnetic measurements or eventually from spectroscopic techniques like inelastic neutron scattering,[24] and the precise nature of these low-lying states as deduced from EPR data. The various theoretical models were then utilized to interpret, qualitatively or quantitatively, these energetic properties. To our knowledge, very few experimental data concern the spatial spin distribution. This paper is devoted to one of the first studies of this kind.

The knowledge about spin distribution in mononuclear coordination compounds has made significant progress in the last 10 years owing to polarized neutron diffraction (PND). This technique allows for the full determination of the spatial distribution of the spin density, over a unique single crystal. As PND is only sensitive to electrons carrying unpaired spins and belonging to the outer valence shell, it provides a direct test for metal–ligand bonding. The determination of the spin delocalization on the ligands allows for detailed studies of covalency in coordination compounds.

About 10 complexes of first-row transition ions have been investigated thus far, with different kinds of ligands: monoatomic ligands in $CoCl_4^{2-}$,[25,26] $CoBr_4^{2-}$,[27] and CrF_6^{3-},[28] polyatomic ligands in $Cr(CN)_6^{3-}$,[29] $Fe(CN)_6^{3-}$,[30] $Mn(H_2O)_6^{2+}$,[31] $Ni(H_2O)_6^{2+}$,[32] and $Ni(NH_3)_4(NO_2)_2$[33] macrocycles in CoPc[34] and MnPc[35] with Pc = phthalocyaninato. A recent paper reports on a compound with two different Fe(III) complexes in the same lattice, namely, $\{Fe(bipy)_2Cl_2\}^+$ and $(FeCl_4)^-$.[36,37] Combined charge and spin density studies on a given compound offer a unique test for the electronic wave function and are now systematically performed.[26,29,33,37,38]

The PND technique is also a unique tool to study magnetic materials. For instance, superexchange through Cl^- bridges between Cr(II) ions separated by more than 5 Å has been demonstrated by PND in Rb_2CrCl_4, which exhibits a ferromagnetic ordering.[39] Applied to polymetallic molecular compounds, PND should yield useful information on the exchange interaction mechanism. However, to our knowledge, only one study of this kind has appeared so far, dealing with a ferromagnetically coupled hydroxo-bridged copper(II) dimer.[40] No PND study concerns heteropolymetallic systems.

In this paper, we report on a PND study dealing with the heterodinuclear compound Cu(salen)Ni(hfa)$_2$ with salen = *N*,*N'*-ethylenebis(oxosalicyldiiminato) and hfa = hexafluoroacetylacetonato. A short communication on this work has recently been published.[41] In Cu(salen)Ni(hfa)$_2$, the intramolecular antiferromagnetic interaction gives rise to a ground doublet and an excited quartet pair state with a doublet–quartet energy gap of 35.4 cm^{-1}.[42] The magnetic susceptibility at low temperature is high enough to make possible the measurement of the magnetization density $\rho_M(\vec{r})$, induced by a magnetic field of a few Teslas. PND on a single crystal provides a set of experimental

Table I. Information Concerning Crystallographic Data Collection

Crystallographic and Physical Data		
space group	monoclinic $P2_1/n$	
temp, K	19.6	123.0
a, Å	9.16 (5)	9.287 (4)
b, Å	21.47 (2)	21.533 (2)
c, Å	14.70 (3)	14.733 (3)
β, deg	93.9 (4)	94.36 (3)
V, Å^3	2886 (2)	2937.8 (7)
Z	4	
abs factor, cm^{-1}	0.531	
sample	single crystal	
morphology	dark red	
	max size 6 mm	
	min size 3 mm	

Data Collection	
temp, K	19.6
radiat	neutron
monochromator	copper
λ, Å	0.831
scan mode	ω scan
max Bragg angle, deg	50
no. of steps	35
step width, deg	0.09
counting time/point, s	4
contrl reflcn	(0,7,7)

Condition for Refinement	
no. of reflcns for refinement of cell dimens	16
no. of recorded reflcns	2672
no. of utilized reflcns, $I > 3\sigma$	1731
no. of refined param	378
reliability factor: refinement on F^2	
$R = \sum\|k\|F_o\| - \|F_c\|\|/\sum kF_o^2$	0.049
$RI = \sum\|kF_o^2 - F_c^2\|/\sum kF_o^2$	0.064
$RI_w = [\sum w(kI_o - I_c)^2/\sum w(kI_o)^2]$	0.074
$w = 1/\sigma_o^2$	

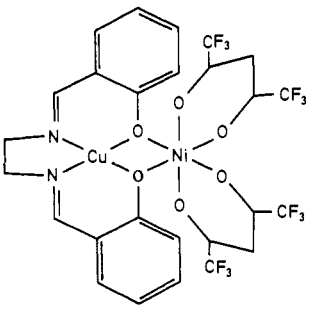

(21) Albonico, C.; Bencini, A. *Inorg. Chem.* **1988**, *27*, 1934.
(22) Scaringe, R. P.; Hodgson, D.; Hatfield, W. E. *Mol. Phys.* **1978**, *35*, 701.
(23) Gatteschi, D.; Bencini, A. in ref 1, p 241, and references therein.
(24) Güdel, H. U. in ref 1, p 329, and references therein.
(25) Chandler, G. S.; Figgis, B. N.; Phillips, R. A.; Reynolds, P. A.; Mason, R.; Williams, G. A. *Proc. R. Soc. London* **1982**, *A384*, 31.
(26) Figgis, B. N.; Reynolds, P. A.; White, A. H. *J. Chem. Soc., Dalton Trans.* **1987**, 1737.
(27) Figgis, B. N.; Reynolds, P. A.; Mason, R. *Proc. R. Soc. London* **1982**, *A384*, 49.
(28) Figgis, B. N.; Reynolds, P. A.; Williams, G. A. *J. Chem. Soc., Dalton Trans.* **1980**, 2348. Mason, R.; Smith, A. R. P; Varghese, J. N. *J. Am. Chem. Soc.* **1981**, *103*, 1300.
(29) Figgis, B. N.; Forsith, J. B.; Mason, R.; Reynolds, P. A. *Chem. Phys. Lett.* **1985**, *115*, 454. Figgis, B. N.; Forsyth, J. B.; Reynolds, P. A. *Inorg. Chem.* **1987** *26*, 101.
(30) Brown, P. J.; Day, P.; Fisher, P.; Güdel, H. U.; Herren, F.; Ludi, A. *J. Phys.* **1982**, *43*, C7-235.
(31) Fender, B. E. F.; Figgis, B. N.; Forsyth, J. B.; Reynolds, P. A.; Stevens, E. *Proc. R. Soc. London* **1986**, *A404*, 127.
(32) Fender, B. E. F.; Figgis, B. N.; Forsyth, J. B. *Proc. R. Soc. London* **1986**, *A404*, 139.
(33) Chandler, G. S.; Figgis, B. N.; Phillips, R. A.; Reynolds, P. A.; Mason, R. *J. Phys.* **1982**, *43*, C7-323.
(34) Williams, G. A.; Figgis, B. N.; Mason, R. *J. Chem. Soc., Dalton Trans.* **1981**, 734.
(35) Figgis, B. N.; Williams, G. A.; Forsyth, J. B.; Mason, R. *J. Chem. Soc., Dalton Trans.* **1981**, 1837.
(36) Figgis, B. N.; Reynolds, P. A.; White, A. H. *Inorg. Chem.* **1985**, *24*, 3762.
(37) Figgis, B. N.; Reynolds, P. A.; Forsyth, J. B. *J. Chem. Soc., Dalton Trans.* **1988**, 117.
(38) Becker, P.; Coppens, P. *Acta Crystallogr.* **1985**, *A41*, 177.
(39) Day, P.; Fyne, P. J.; Hellner, E.; Hutchings, M. T.; Munninghoff, G.; Tasset, F. *Proc. R. Soc. London* **1986**, *A406*, 39.
(40) Figgis, B. N.; Mason, R.; Smith, A. R. P.; Varghese, J. N.; Williams, G. A. *J. Chem. Soc., Dalton Trans.* **1983**, 703.
(41) Gillon, B.; Journaux, Y.; Kahn, O. *J. Phys.* **1988**, *46*, C8-863. *Physica B* **1989**, *156–157*, 373.
(42) Journaux, Y.; Kahn, O.; Morgenstern-Badarau, I.; Galy, J.; Jaud, J.; Bencini, A.; Gatteschi, D. *J. Am. Chem. Soc.* **1985**, *107*, 6305.

magnetic structure factors $F_M(hkl)$, Fourier components of $\rho_M(\vec{r})$, which permits determination of the spin density distribution $\rho_M(\vec{r})$ in the whole space.

The paper is organized as follows. The structure at 19.6 K of Cu(salen)Ni(hfa)$_2$, obtained by unpolarized neutron diffraction, is briefly described. Then, the results of the PND experiment are reported and interpreted in terms of spin distribution maps and of atomic spin populations on the metals and their eight nearest neighbors. A theoretical interpretation of the PND data is proposed. Finally, a thorough discussion is presented.

Experimental Section and Calculation Method

Synthesis. Cu(salen)Ni(hfa)$_2$ was synthesized as previously described.[42] Large and well-shaped single crystals were obtained by slow evaporation of a saturated solution of Cu(salen)Ni(hfa)$_2$ in chloroform containing small monocrystalline seeds of Cu(salen)Ni(hfa)$_2$.

Structure Determination at 19.6 K through Neutron Diffraction. In order to determine the atomic positions and thermal parameters at low temperature, including those of the hydrogen atoms, we performed an unpolarized neutron experiment at the Laboratoire Léon Brillouin on the four-circle diffractometer 5C2. The experimental and refinement conditions are summarized in Table I. The crystallographic structure was known from X-ray diffraction at 123 K.[42] The space group is $P2_1/n$ with $Z = 4$. The cell parameters refined from 16 reflections are given in Table I. No equivalent reflections were recorded. Lorentz factors were applied. Absorption corrections were performed by assuming a regular block shape with the three faces perpendicular to the main crystallographic axes. Only reflections with $I > 3\sigma$ were used in the refinement. The structure at 19.6 K was refined by using the position and thermal parameters of the structure at 123 K as initial parameters. The data at 123 K displayed some disorder of the fluorine atoms over three crystallographic independent positions, with different occupancy factors. After cooling down, the fluorine atoms were found to be frozen in the positions corresponding to the highest occupancy factor. Only 24 atoms including the Cu, Ni, and bridging oxygen atoms were allowed to refine with anisotropic thermal parameters. A reliability factor of 0.049 was obtained. The atomic position and thermal parameters are listed in Table II.

Polarized Neutron Experiment. The polarized neutron diffraction technique consists of measuring the flipping ratio $R(hkl)$ at the peak of each Bragg reflection of a crystal. $R(hkl)$ is defined as the ratio between the intensities diffracted when the neutron beam is polarized parallely $[(I_\uparrow(hkl)]$ and antiparallely $[(I_\downarrow(hkl)]$, respectively, to the vertical magnetic field:

$$R(hkl) = I_\uparrow(hkl)/I_\downarrow(hkl) \quad (1)$$

In the case of a centrosymmetrical crystal, the experimental value of this flipping ratio permits direct determination of the value of the ratio $\gamma = (F_M/F_N)$ between the magnetic and nuclear structure factors of the Bragg reflection, from the equation

$$R(hkl) = (1 + 2pq^2\gamma + q^2\gamma^2)/(1 - 2peq^2 + q^2\gamma^2) \quad (2)$$

where p is the beam polarization, e the flipping efficiency ($e = 1.0$ for the cryoflipping device we utilized), and $q^2 = \sin^2\alpha$, α being the angle between the induced magnetic momentum and the Bragg scattering vector.

The experiment was performed on the normal beam-polarized neutron diffractometer 5C1 at the Laboratoire Léon Brillouin (reactor Orphée located at Saclay, France, of which the power is 14 MW). The experimental conditions are indicated in Table III. The sample was a regularly shaped dark red single crystal. Its dimensions were $8 \times 3 \times 2$ mm^3, with the long dimension along the a axis. The experimental conditions of temperature (2 K) and of magnetic field (5×10^4 G) obtained by a superconducting cryomagnet were chosen in order to approach the saturation magnetization, i.e., 1.15 μ_B mol^{-1}.

Two separate sets of data were collected for two different orientations of the crystal with respect to the magnetic field, at $\lambda = 0.730$ and 0.865 Å, respectively. The neutron beam polarization is then equal to 0.972 (4) and 0.976 (4), respectively. An Erbium filter (absorption maximum between 0.73 and 0.90 Å) was used in order to eliminate most of the $\lambda/2$ contribution. The crystal was first mounted with the a axis vertical, and 200 reflections $0kl$ were measured within $(\sin\theta)/\lambda = 0.50$ Å^{-1}. It was then mounted with the b axis vertical, and 652 reflections h,k,l with $k = 0, 1, 2$ were measured within $(\sin\theta)/\lambda = 0.53$ Å^{-1}. Averaging the reflections measured more than once and the equivalent reflections provides two sets of 76 and 212 independent reflections, respectively, with $|F| > 2\sigma$, including 11 reflections common to both data collections.

For each reflection, eq 2 was solved, giving the γ value. The choice of the solution is generally obvious. The magnetic structure factor was then deduced from γ and the value of F_N calculated from the low-temperature crystal structure.

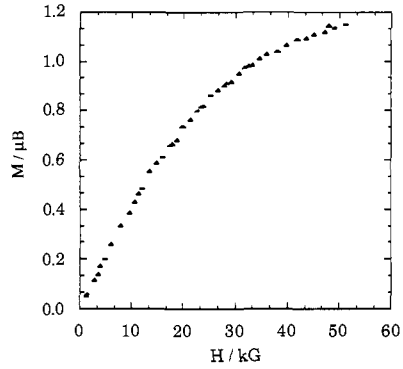

Figure 1. Magnetization vs external magnetic field plot at 2 K for Cu(salen)Ni(hfa)$_2$.

Magnetization. The magnetization was measured at 2 K and in the $(0-5) \times 10^4$ G external magnetic field range with a laboratory-made apparatus working according to the extraction method. The curve is shown in Figure 1. At 5×10^4 G, the magnetization is equal to 1.15 μ_B mol^{-1} (or 6700 cm^3 mol^{-1} G), which is close to the expected saturation magnetization $M_S = (^1/_2)N\beta g_{1/2}$, where $g_{1/2}$ is the Zeeman factor associated with the doublet ground doublet state.

Molecular Orbital Calculations. They were performed by using the FORTICON 8 version of the extended Hückel program for the hypothetical complex of which the atomic coordinates are given in Table SVIII. The calculations were carried out in two steps, the former concerning the ligands, the latter the dinuclear complex as a whole. A charge iteration procedure including Madelung corrections was used for phenolato and 1,2-ethanediimine ligands in order to optimize the H_{ii}'s parameters for oxygen, nitrogen, and carbon atoms. For hexafluoroacetylacetonato, a slightly more complicated approach was used, consisting first of consideration of the CF_3 group, to determine the H_{ii} parameters for the carbon atom in CF_3, then of performance of the calculation for the acetylacetonato ligand replacing the CF_3 group by a carbon atom. The calculations for the binuclear compound were performed without charge iteration and with the corrected H_{ii} values extracted from the previous calculations. All the parameters used for these calculations are given in Tables SIX and SX.

Description of the Structure at 19.6 K

A perspective view of the Cu(salen)Ni(hfa)$_2$ unit is shown in Figure 2. A list of selected bond lengths and angles is given in Table IV, in comparison with the values obtained at 123 K. The bond lengths are very weakly modified between these two temperatures. The copper environment is almost square planar, with Cu–O and Cu–N lengths very close to each other, ranging from 1.90 to 1.92 Å. The bond angles slightly deviate from 90° in quite a symmetrical way, the O_1CuO_2 and N_5CuN_6 angles being both contracted and equal to 83.6 and 85.7°, respectively. The nickel atom is in a slightly distorted octahedral configuration with Ni–O lengths ranging from 2.00 to 2.10 Å. The ONiO bond angles are distributed over a range from 75.4 to 102.3°. The CuO_1O_2Ni bridging network is significantly bent around the O_1O_2 direction; the O_1CuO_2 and O_1NiO_2 planes make a dihedral angle equal to 142.7°. The bridging angles CuO_1Ni and CuO_2Ni are equal to 94.56 and 92.48°, respectively. The Cu···Ni separation is equal to 2.906 (5) Å.

Determination of the Spin Density

The experimental magnetic structure factors $F_M(K)$ yielded by the PND experiment are related to the magnetization density $\rho_M(\vec{r})$ through a Fourier transformation:

$$F_M(\vec{K}) = \int_{cell} \rho_M(\vec{r}) \exp(i\vec{K}\cdot\vec{r})\, d\vec{r} \quad (3)$$

The magnetization density $\rho_M(\vec{r})$ integrated over the crystallographic cell is equal to the magnetization corresponding to the four molecules of the asymmetric unit, i.e., $M = 4 \times 1.15$ μ_B at 2 K and under 5×10^4 G. The magnetic structure factors are here expressed in Bohr magnetons μ_B.

Strickly speaking, the magnetization density is the sum of two contributions, namely, the spin density reflecting the spin dis-

Table II. Atomic Positions and Thermal Parameters (Å^2) for Cu(salen)Ni(hfa)$_2$ Determined by Neutron Diffraction at 19.6 K

	x/a	*y/b*	*z/c*	*B*		*x/a*	*y/b*	*z/c*	*B*
Cu	0.4055 (4)	−0.0101 (1)	0.5962 (2)		H161	0.6719 (10)	−0.1243 (4)	0.7219 (5)	1.74 (15)
Ni1	0.3332 (3)	0.1061 (1)	0.6842 (1)		C62	0.4915 (5)	−0.1354 (2)	0.5772 (2)	0.60 (7)
O1	0.2844 (5)	0.0592 (2)	0.5640 (3)		H162	0.5594 (10)	−0.1325 (4)	0.5191 (5)	1.77 (15)
O2	0.5178 (5)	0.0503 (2)	0.6670 (3)		H262	0.5164 (10)	−0.1783 (4)	0.6137 (5)	
N5	0.2930 (3)	−0.0680 (1)	0.5206 (2)	0.73 (5)	O3	0.2732 (5)	0.0297 (2)	0.7563 (3)	
N6	0.5221 (3)	−0.0801 (1)	0.6334 (2)	0.51 (5)	O4	0.3890 (5)	0.1504 (2)	0.8022 (3)	
C11	0.1897 (5)	0.0629 (2)	0.4923 (2)	0.57 (7)	O5	0.1356 (5)	0.1467 (2)	0.6883 (3)	0.47 (7)
C12	0.1336 (5)	0.1224 (2)	0.4666 (2)	0.61 (7)	O6	0.4139 (5)	0.1805 (2)	0.6224 (3)	0.49 (7)
H112	0.1685 (10)	0.1631 (4)	0.5062 (5)	1.79 (15)	C1	0.3032 (4)	0.0230 (2)	0.8404 (2)	0.51 (7)
C13	0.0367 (5)	0.1284 (2)	0.3899 (2)	0.59 (7)	C2	0.3496 (5)	0.0674 (2)	0.9052 (2)	0.69 (7)
H113	−0.0020 (10)	0.1748 (3)	0.3707 (5)		H12	0.3623 (11)	0.0535 (4)	0.9751 (5)	
C14	−0.0118 (5)	0.0761 (2)	0.3381 (2)	0.75 (7)	C3	0.3830 (5)	0.1283 (2)	0.8800 (2)	0.34 (6)
H114	−0.0854 (10)	0.0814 (4)	0.2810 (5)	2.10 (15)	C4	0.2800 (5)	−0.0441 (2)	0.8746 (2)	0.41 (7)
C15	0.0407 (5)	0.0178 (2)	0.3639 (2)	0.66 (7)	C5	0.4259 (5)	0.1758 (2)	0.9560 (2)	0.59 (7)
H115	0.0050 (10)	−0.0223 (4)	0.3262 (5)	1.85 (15)	C6	0.1203 (5)	0.2049 (2)	0.6838 (2)	0.48 (7)
C16	0.1451 (5)	0.0099 (2)	0.4395 (2)	0.65 (7)	C7	0.2173 (5)	0.2502 (2)	0.6542 (2)	0.66 (7)
C21	0.6192 (5)	0.0359 (2)	0.7326 (2)	0.64 (7)	H17	0.1837 (10)	0.2974 (5)	0.6523 (4)	
C22	0.6895 (5)	0.0851 (2)	0.7816 (2)	0.70 (7)	C8	0.3554 (5)	0.2340 (2)	0.6250 (2)	0.66 (7)
H122	0.6596 (10)	0.1328 (4)	0.7619 (5)	1.60 (15)	C9	−0.0297 (5)	0.2268 (2)	0.7122 (2)	0.68 (7)
C23	0.7913 (5)	0.0743 (2)	0.8533 (2)	0.68 (7)	C10	0.4467 (5)	0.2875 (2)	0.5912 (2)	0.58 (7)
H123	0.8417 (10)	0.1118 (4)	0.8906 (5)		F14	0.3196 (5)	−0.0865 (2)	0.8138 (3)	
C24	0.8317 (5)	0.0126 (2)	0.8785 (2)	0.84 (7)	F24	0.1397 (6)	−0.0531 (2)	0.8879 (3)	1.01 (9)
H124	0.9091 (11)	0.0043 (4)	0.9332 (6)		F34	0.3570 (6)	−0.0560 (2)	0.9532 (3)	
C25	0.7677 (5)	−0.0366 (2)	0.8283 (2)	0.53 (7)	F15	0.3424 (6)	0.2267 (2)	0.9453 (3)	
H125	0.8011 (10)	−0.0833 (4)	0.8438 (5)	2.02 (15)	F25	0.4089 (6)	0.1539 (2)	1.0385 (3)	1.22 (9)
C26	0.6623 (5)	−0.0259 (2)	0.7553 (2)	0.51 (7)	F35	0.5644 (6)	0.1938 (2)	0.9523 (3)	
C51	0.1920 (5)	−0.0528 (2)	0.4591 (2)	0.51 (7)	F19	−0.0440 (6)	0.2889 (2)	0.7114 (3)	
H151	0.1387 (10)	−0.0894 (4)	0.4184 (5)	1.94 (15)	F29	−0.1382 (6)	0.2038 (2)	0.6568 (3)	
C52	0.3305 (5)	−0.1326 (2)	0.5413 (2)	0.69 (7)	F39	−0.0505 (6)	0.2079 (2)	0.7968 (3)	
H152	0.2597 (10)	−0.1485 (4)	0.5948 (5)		F110	0.5026 (6)	0.3217 (2)	0.6622 (3)	
H252	0.3102 (10)	−0.1618 (3)	0.4809 (5)		F210	0.3693 (6)	0.3259 (2)	0.5363 (3)	
C61	0.6184 (5)	−0.0803 (2)	0.7022 (2)	0.84 (7)	F310	0.5610 (6)	0.2674 (2)	0.5464 (3)	

	$\beta(1, 1)$	$\beta(2, 2)$	$\beta(3, 3)$	$\beta(2, 3)$	$\beta(1, 3)$	$\beta(1, 2)$
Cu	0.0018 (7)	0.0002 (1)	0.0006 (2)	0.0001 (1)	−0.0004 (3)	0.0000 (2)
Ni1	0.0018 (7)	0.0002 (1)	0.0004 (2)	0.0001 (1)	−0.0002 (3)	0.0001 (2)
O1	0.0027 (7)	0.0002 (1)	0.0007 (2)	−0.0001 (1)	−0.0008 (3)	0.0001 (2)
O2	0.0018 (7)	0.0002 (1)	0.0004 (2)	−0.0002 (1)	−0.0002 (3)	0.0002 (2)
H113	0.0076 (13)	0.0006 (2)	0.0019 (3)	−0.0001 (2)	−0.0002 (6)	0.0005 (4)
H123	0.0081 (14)	0.0011 (2)	0.0022 (3)	−0.0001 (2)	−0.0018 (6)	0.0009 (4)
H124	0.0087 (14)	0.0010 (2)	0.0027 (4)	−0.0001 (2)	−0.0014 (6)	−0.0004 (4)
H152	0.0037 (13)	0.0009 (2)	0.0028 (4)	0.0007 (2)	−0.0002 (6)	−0.0002 (4)
H252	0.0042 (12)	0.0006 (2)	0.0028 (4)	−0.0004 (2)	−0.0012 (5)	0.0004 (2)
H262	0.0076 (13)	0.0006 (2)	0.0019 (3)	0.0003 (2)	−0.0001 (5)	0.0008 (4)
O3	0.0022 (7)	0.0002 (1)	0.0005 (2)	0.0002 (1)	−0.0001 (3)	0.0002 (2)
O4	0.0016 (7)	0.0002 (1)	0.0004 (2)	0.0001 (1)	−0.0005 (3)	0.0001 (2)
H12	0.0101 (15)	0.0007 (2)	0.0026 (4)	0.0000 (2)	−0.0012 (6)	−0.0003 (4)
H17	0.0038 (12)	0.0008 (2)	0.0028 (3)	−0.0005 (2)	0.0008 (5)	−0.0001 (4)
F14	0.0025 (7)	0.0000 (1)	0.0009 (2)	−0.0001 (1)	0.0002 (3)	0.0000 (2)
F34	0.0042 (8)	0.0002 (1)	0.0011 (2)	0.0002 (1)	−0.0006 (3)	0.0001 (2)
F15	0.0039 (7)	0.0003 (1)	0.0008 (2)	−0.0003 (1)	−0.0007 (3)	0.0007 (2)
F35	0.0029 (8)	0.0007 (1)	0.0013 (2)	−0.0004 (1)	−0.0005 (3)	0.0001 (2)
F19	0.0022 (7)	0.0001 (1)	0.0014 (2)	0.0001 (1)	0.0000 (3)	0.0004 (2)
F29	0.0037 (8)	0.0006 (1)	0.0014 (2)	−0.0006 (1)	−0.0004 (3)	0.0002 (2)
F39	0.0042 (8)	0.0005 (1)	0.0014 (2)	0.0003 (1)	0.0007 (3)	0.0005 (2)
F110	0.0048 (8)	0.0005 (1)	0.0012 (2)	−0.0001 (1)	−0.0006 (3)	−0.0006 (2)
F210	0.0039 (8)	0.0005 (1)	0.0010 (2)	0.0005 (1)	−0.0005 (3)	0.0001 (2)
F310	0.0049 (8)	0.0004 (1)	0.0023 (2)	0.0002 (1)	0.0020 (3)	−0.0004 (2)

Table III. Information Concerning the Polarized Neutron Diffraction Data Collection

temp, K	2	
field	5×10^4 G	
sample	single crystal $8 \times 3 \times 2$ mm^3	
morphology	dark red block	
vertical axis	*a*	*b*
wavelength, Å	0.730	0.865
$(\sin\theta)/\lambda_{max}$	0.497	0.433
no. of reflcns measd	200	652
no. of indepnt reflcns	81	256
$\|F\| > 2\sigma$	76	212

tribution of the unpaired electrons, and the orbital momentum density, corresponding to the magnetic momenta created by the rotation of the unpaired electrons on their orbit around the direction of the applied magnetic field. This latter contribution is negligible when the interacting magnetic centers have no first-order angular momentum. This is the case for the nickel(II) ion in octahedral surroundings and copper(II) in square-planar surroundings. In the following, we will relate the magnetization density obtained from PND to the spin density, which will be expressed in μ_B Å^{-3}.

Fourier Summation. A first way to deduce the spin density from the experimental magnetic structure factors $F_M(hkl)$ is to perform a Fourier summation of these $F_M(hkl)$'s, which is mathematically correct for an infinite series with h,k,l taking all integer values from $-\infty$ to $+\infty$:

$$\rho(x,y,z) = (1/V) \sum_{h,k,l=-\infty}^{+\infty} F_M(h,k,l) \exp[-i(hx + ky + lz)] \quad (4)$$

where V is the cell volume. Truncation of the Fourier series

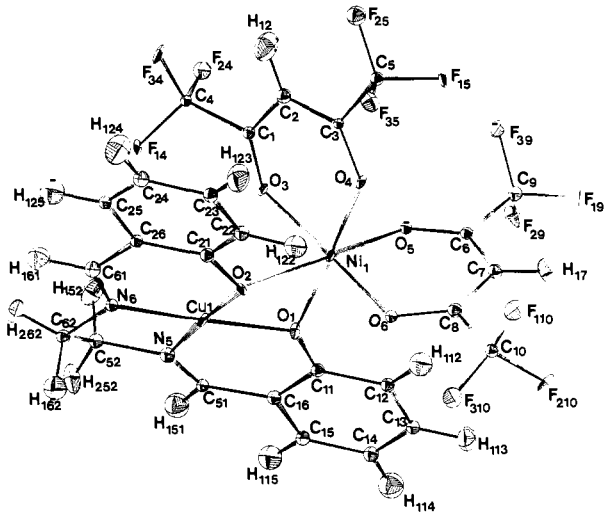

Figure 2. Perspective view of Cu(salen)Ni(hfa)$_2$ at 19.6 K.

Table IV. Bond Lengths and Angles for Cu(salen)Ni(hfa)$_2$ at 123 K (from X-ray Diffraction) and 19 K (from Neutron Diffraction)

	123 K	19 K
	Bond Lengths	
Cu1O1	1.892 (2)	1.897 (1)
Cu1O2	1.908 (2)	1.918 (12)
Cu1N5	1.914 (3)	1.921 (10)
Cu1N6	1.904 (3)	1.903 (1)
Cu1Cu'1	3.432 (2)	3.441 (5)
Cu1Ni1	2.897 (2)	2.906 (5)
NiO1	2.064 (2)	2.056 (10)
NiO2	2.107 (2)	2.102 (2)
NiO3	2.043 (2)	2.048 (5)
NiO4	2.011 (2)	2.014 (10)
NiO5	2.011 (2)	2.015 (4)
NiO6	2.011 (2)	2.003 (4)
	Bond Angles	
O1-Cu1-O2	83.9 (1)	83.6 (3)
O2-Cu1-N6	95.6 (1)	96.2 (3)
N6-Cu1-N5	86.3 (1)	85.7 (2)
N5-Cu1-O1	94.2 (1)	94.6 (4)
O1-Cu1-N6	177.4 (1)	177.3 (1)
O2-Cu1-N5	177.5 (1)	177.4 (1)
Cu1-O1-Ni1	94.08 (8)	94.56 (70)
Cu1-O2-Ni1	93.70 (8)	92.48 (30)
O5-Ni1-O1	96.1 (1)	95.4 (4)
O5-Ni1-O2	169.7 (1)	169.3 (6)
O5-Ni1-O3	93.3 (1)	93.3 (2)
O5-Ni1-O4	86.9 (1)	86.9 (2)
O5-Ni1-O6	91.2 (1)	91.6 (1)
O4-Ni1-O1	177.0 (1)	177.7 (2)
O4-Ni1-O2	102.0 (1)	102.3 (4)
O4-Ni1-O3	90.0 (1)	89.6 (1)
O4-Ni1-O6	86.0 (1)	86.2 (4)
O6-Ni1-O1	93.8 (1)	93.8 (1)
O6-Ni1-O2	94.5 (1)	94.3 (1)
O6-Ni1-O3	173.8 (1)	173.4 (5)
O3-Ni1-O1	89.9 (1)	90.1 (4)
O3-Ni1-O2	81.6 (1)	81.5 (1)
O1-Ni1-O2	75.1 (1)	75.4 (2)

introduces spurious oscillations in the density map. In order to reduce these truncation effects, one can average the density over a small volume around each considered point. This corresponds to minimizing the relative weight of the missing factors at the end of the series with regard to the factors used in the Fourier summation.[43] On the other hand, such a procedure does not compensate the errors due to terms missing in the explored domain $[(\sin\theta)/\lambda]_{max}$ of the reciprocal space. A significant percentage, which can reach 50%, of the $F_M(hkl)$ factors in this domain may

(43) Shull, C. G.; Mook, H. A. *Phys. Rev. Lett.* **1966**, *16*, 184.

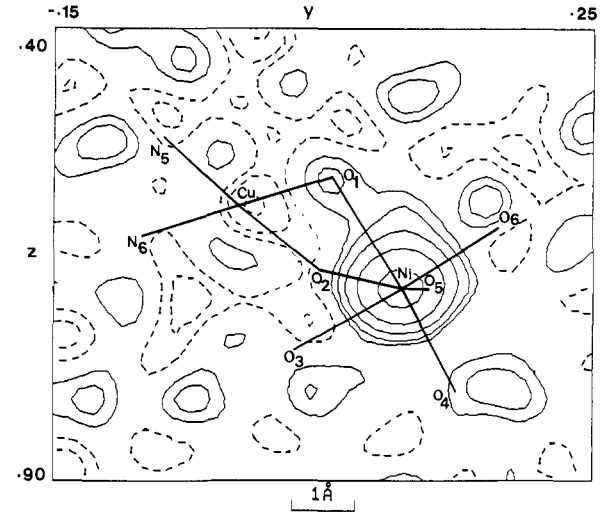

Figure 3. Fourier projection along the crystallographic axis a of the experimental magnetization density. The positive contours (continuous lines) are $0.005 \times 2^{n-1}$ μ_B Å^{-2} with n = 1–5, and the negative contours (dotted lines) are $-0.005 \times 2^{n-1}$ μ_B Å^{-2} with n = 1–3.

be impossible to determine because the corresponding nuclear reflections are too weak to enable measurement of the flipping ratios with good accuracy in a reasonable counting time. This is true even for low h,k,l values. These errors are responsible for substantial distortions of the spin density map.

The projection of the spin density along the a axis onto the (b, c^*) plane obtained from 81 $F_M(0kl)$ magnetic structure factors is shown in Figure 3. The $F_M(000)$ term, equal to the experimental magnetization value in the cell (4.56 μ_B), has been included in the summation. Most of the spin density appears to be located around the nickel atom. A region of negative spin density is also observed around the copper atom. Regarding the distortions of the map due to the lack of 70% of the $F_M(0kl)$ factors in the domain $(\sin\theta)/\lambda < 0.5$ Å^{-1}, it is not possible to estimate the spin delocalization on the ligands. A projection along the b axis onto the (a, c) plane also shows a strong positive density around the nickel atom and a weak negative spin density around the copper atom.

Spin Density Modeling. A second way to visualize the spin density consists of fitting the experimental magnetic structure factors by refining the parameters of a spin density model and using the final parameters to represent the spin density. Such an approach is close to that used to determine the charge densities. Actually, the spin density and the charge density problems are formally similar. Of course, the former only takes into account the singly occupied orbitals, whereas the latter takes into account all occupied orbitals. We will use the multipole model.[44] This model consists of expressing the total spin density $\rho_M(\vec{r})$ as a sum of atomic densities, developed on the basis of spherical harmonics centered on each atom i, with population coefficients P_{lm}:

$$\rho_M(\vec{r}) = \sum_i \sum_{l=0}^{\infty} \sum_{m=-1}^{+1} P_{lm} \rho^i_{lm}(\vec{r}) \qquad (5)$$

Each multipolar function is the product of a Slater-type radial function $R_l^i(r)$, depending only on l, and written as

$$R_l^i(r) = [\zeta_l^{n_l+3}/(n_l + 2)!] r^{n_l} \exp(-\zeta_l r) \qquad (6)$$

by a real spherical harmonics:

$$y_{lm+}(r) = \tfrac{1}{2}(Y_{lm+} + Y_{lm-})$$
$$y_{lm-}(r) = 1/2i(Y_{lm+} - Y_{lm-}) \qquad (7)$$

where Y_{lm} is the classical spherical harmonics. The Fourier

(44) Brown, P. J.; Capiomont, A.; Gillon, B.; Schweizer, J. *J. Magn. Magn. Mater.* **1979**, *14*, 289.

Table V. Values of the Refined Multipole Parameters on $n_o = 277$ Experimental Structure Factors with $|F_M| > 2\sigma^a$

	1	2
n_v variables	12	16
ζ_{Cu}, au^{-1}	8.8 (7)	9.07 (14)
P_{00}	−0.249 (10)	−0.250 (10)
P_{20}		−0.033 (44)
P_{40}		−0.126 (100)
P_{44}		−0.062 (136)
ζ_{Ni}, au^{-1}	8.89 (13)	9.07 (14)
P_{00}	1.262 (11)	1.259 (11)
P_{40}		0.115 (85)
P_{00}(O1)	0.020 (10)	0.006 (10)
P_{00}(O2)	−0.003 (10)	−0.003 (10)
P_{00}(O3)	0.029 (9)	0.039 (9)
P_{00}(O4)	0.027 (9)	0.027 (9)
P_{00}(O5)	0.043 (10)	0.039 (9)
P_{00}(O6)	0.024 (9)	0.034 (9)
P_{00}(N5)	−0.024 (9)	−0.017 (11)
P_{00}(N6)	−0.010 (10)	−0.003 (10)
R^b	0.0915	0.0858
χ^c	1.466	1.417

[a] Column 1 corresponds to spherical monopole refinement and column 2 to the final multipole refinement. [b] $R = [\sum(F_o - F_c)^2/\sigma^2]^{1/2}/\sum F_o^2/\sigma_o^2$. [c] $\chi = [[\sum(F_o - F_c)^2/\sigma^2]/(n_o - n_v)]^{1/2}$.

transform of expression 5 yields the following parametrical expression for the structure factors:

$$F_M(\vec{K}) = \sum_i [\sum_{l=0}^{\infty} \psi_l^i(K) \sum_{m=-1}^{+1} p_{lm} y_{lm}(K)] \exp(-i\vec{K}\cdot\vec{r}_i) \exp(-W_i) \quad (8)$$

with

$$\psi_l^i(K) = i^l \int_0^\infty R_l^i(r) j_l(Kr) r^2 \, dr \quad (9)$$

where $j_l(Kr)$ is a spherical Bessel function. The parameters are the populations P_{lm} and the radial Slater exponents ζ_l for each atom. They are refined by comparing the experimental values of the magnetic structure factors to those derived from eq 8. The radial function coefficients n_l and ζ_l are chosen by analogy of the multipole density functions with products of atomic orbitals. This is obvious for the case of a transition metal with only one unpaired electron in a 3d atomic orbital, the square of which corresponds to the spin density $\rho(r)$ in a restricted Hartree–Fock scheme. From the products of 3d functions arise multipolar functions with $n_l = 4$ and $\zeta_l = 2\alpha_{3d}$ for all l values, α_{3d} being the Slater exponent of the atomic orbital. We made the choice of larger values of n_l for octopoles and hexadecapoles ($n_3 = 6$ and $n_4 = 8$, respectively), which actually gives better refinements.[45] By analogy, the same kind of multipolar function is used for nickel(II) with two unpaired electrons. Similarly, the choice of the radial parameters for nitrogen and oxygen atoms gives $n_{1,2} = 2$, $n_3 = 3$, and $n_4 = 4$, with $\zeta_l = 2\alpha_{2p}$.

The multipolar expansion of the spin density has been restricted to the metal ions and their eight nearest neighbors. Starting values of Slater exponents for the metal atoms[46] were $\zeta_{Cu} = 8.80$ au^{-1} and $\zeta_{Ni} = 8.35$ au^{-1}, and for light atoms[47] $\zeta_N = 3.90$ au^{-1} and $\zeta_O = 4.50$ au^{-1}. Multipoles up to $l = 4$ (hexadecapoles) have been introduced for the metal atoms. Constraints based on the local symmetry have been applied; the copper and nickel environments were assumed to be strictly square planar and octahedral, respectively. The mutlipole basis is then reduced[48] to y_{00}, y_{20}, y_{40} and y_{44+} for copper, and y_{00}, y_{40}, and y_{44+} for nickel, with the constraint $P_{44+} = 0.7403P_{40}$. Monopoles have only been refined for the bridging oxygen atoms and the nitrogen atoms bonded to copper. On the other hand, we have assumed that the spin density around each of the four terminal oxygen atoms O_3–O_6 was described by a $2p_z$-type orbital pointing along the Ni–O direction. This assumption corresponds to imposing the constraint $P_{20} = 0.385P_{00}$ to the monopole y_{00} and quadrupole y_{20} functions.

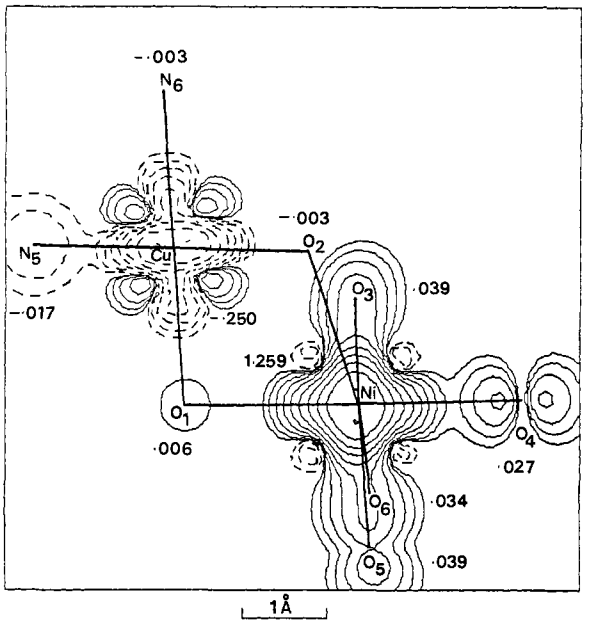

Figure 4. Projection along the direction perpendicular to the CuO_1Ni plan of the spin density obtained by multipole refinement. The contours are the same as in Figure 3, with $n = 1$–9 for the positive contours (maximal 1.28 μ_B Å^{-2}) and $n = 1$–7 for the negative contours (minimal −0.32 μ_B Å^{-2}). The monopole populations in μ_B are indicated for each atom. The uncertainty is 0.01 μ_B.

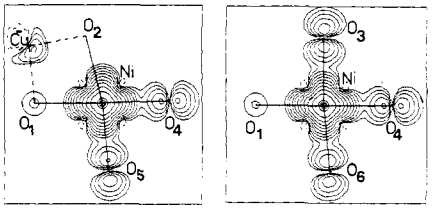

Figure 5. Sections of the spin density in μ_B Å^{-3} from multipole refinement. Left: in the x, y plane of the nickel atom, defined by the NiO_1, NiO_2 bonds. Right: in the y, z plane of the nickel atom, defined by the NiO_1, NiO_3 bonds. The contours correspond to $\pm 0.005 \times 2^{n-1}$ μ_B Å^{-3}. The maximal contour is 2.56 μ_B Å^{-3}.

The results of the first refinement limited to monopole functions on all atoms as well as those of the final refinement are given in Table V. The values of the spherical monopole populations are nothing but the values of the atomic spin populations. The sum of these atomic spin populations is equal to 1.13 μ_B, which agrees very well with the measured magnetization i.e., 1.15 μ_B mol^{-1}. The nickel atom carries 110% of the total momentum, from which a negative contribution of 22% carried by the copper atom has to be subtracted. The spin delocalization on the four terminal oxygen atoms bonded to nickel amounts 12% of the total momentum. In contrast, the delocalization on the bridging oxygen atoms represents less than 1% of the total, which is within the uncertainty on each atomic spin density, estimated at 0.01 μ_B.

The projection of the spin density along the axis perpendicular to the CuO_1Ni plane, obtained from the final mutlipole refinement, is represented in Figure 4. On this figure, the spin density relative to the O_3 and O_6 atoms is superimposed on that relative to the nickel atom. The dissymmetry between bridging and terminal oxygen atoms clearly appears in the map of Figure 4, as well as on the two sections of the spin density through the (x, y) and (y, z) planes relative to the nickel atom (Figure 5). These section maps have to be seen in keeping in mind that we have imposed a σ covalency between $2p_\sigma$ oxygen orbitals and $d_{x^2-y^2}$ (Figure 5, left) and d_{z^2} (Figure 5, right) nickel orbitals.

(45) Hansen, N. K.; Coppens, P. *Acta Crystallogr.* **1978**, *A34*, 909.
(46) Clementi, E.; Raimondi, D. L. *J. Chem. Phys.* **1963**, *38*, 2686.
(47) Hehre, W. J.; Stewart, R. F.; Pople, J. A. *J. Chem. Phys.* **1969**, *51*, 2657.
(48) Holladay, A.; Leung, P.; Coppens, P. *Acta Crystallogr.* **1983**, *A39*, 377.

Theoretical Interpretation

In Cu(salen)Ni(hfa)$_2$, the interaction between the two magnetic centers characterized by $S_{Cu} = {}^1/_2$ and $S_{Ni} = 1$ gives rise to a ground doublet and an excited quartet pair states, with a doublet–quartet energy gap[42] equal to 35.4 cm^{-1}. At the temperature where the polarized neutron study was carried out, i.e., 2 K, only the ground doublet state is thermally populated, so that the spin density obtained corresponds to this ground state. Owing to the bending of the molecule along the direction joining the two bridging oxygen atoms, the exchange interaction in Cu(salen)Ni(hfa)$_2$ is relatively weak. The doublet–quartet energy gap is actually much smaller than in Cu(II)Ni(II) dinuclear compounds with a planar CuO_2Ni bridging network.[49,50] The Heitler–London formalism is then expected to be well adapted to the description of the low-lying states.[8] In this formalism, the wave functions are constructed as products of the magnetic orbitals, the three unpaired electrons occupying these orbitals being the only active electrons of the problem.

Let us define by φ_1 the magnetic orbital centered on copper(II), and by φ_2 and φ_3 the two magnetic orbitals centered on nickel(II). The Heitler–London wave function Ψ_+ associated with the $M_S = {}^1/_2$ component of the doublet pair state is easily obtained through the use of Wigner coefficients[51] as

$$\Psi_+ = 2/6^{1/2}|\bar{\varphi}_1(1)\varphi_2(2)\varphi_3(3)| - 1/6^{1/2}|\varphi_1(1)\bar{\varphi}_2(2)\varphi_3(3)| - 1/6^{1/2}|\varphi_1(1)\varphi_2(2)\bar{\varphi}_3(3)| \quad (10)$$

where the bar notes a β spin. Let us S_i be the local spin operator for the atom i of the dinuclear unit. The spin value $\langle S_i \rangle$ on this atom is given by

$$\langle S_i \rangle = \langle \Psi_+ | S_i | \Psi_+ \rangle \quad (11)$$

which may be expressed as a sum of one-electron integrals. This leads to

$$\langle S_i \rangle = {}^1/_3\langle\varphi_1|S_i|\varphi_1\rangle + {}^2/_3\langle\bar{\varphi}_1|S_i|\bar{\varphi}_1\rangle + {}^5/_6\langle\varphi_2|S_i|\varphi_2\rangle + {}^1/_6\langle\bar{\varphi}_2|S_i|\bar{\varphi}_2\rangle + {}^5/_6\langle\varphi_3|S_i|\varphi_3\rangle + {}^1/_6\langle\bar{\varphi}_3|s_i|\bar{\varphi}_3\rangle \quad (12)$$

Let us note now $P_{\mu i}$ the electronic population of the atom i in the magnetic orbital φ_μ. Equation 12 may be written as

$$\langle S_i \rangle = -{}^1/_6P_{1i} + {}^1/_3P_{2i} + {}^1/_3P_{3i} \quad (13)$$

The spin population p_i on the atom i, expressed in Bohr magnetons, is then given by

$$p_i = g_{1/2}\langle S_i \rangle \quad (14)$$

The average value of the Zeeman factor $g_{1/2}$ may be deduced from the magnetic susceptibility data.[42] In the temperature range where only the ground pair state is populated, $\chi_M T$, χ_M being the molar magnetic susceptibility per Cu(II)Ni(II) unit and T the temperature, is expected to be constant and equal to $N\beta^2 g_{1/2}{}^2/4k$. Experimentally, $\chi_M T$ is actually constant below 10 K and equal to 0.49 cm^{-3} mol^{-1} K, which corresponds to $g_{1/2} = 2.30$.

The problem at hand now is to determine the magnetic orbitals φ_μ, $\mu = 1$–3. To date, two different approaches have been proposed to define the magnetic orbitals;[2,52] the former is that of the orthogonalized magnetic orbitals (OMO). For a dinuclear compound in which the two interacting centers are related through a symmetry element, the method to construct these OMOs is well established. It consists of localizing the singly occupied molecular orbitals for the pair state of highest spin multiplicity. On the other hand, the situation is much more complicated for the dissymmetrical systems like the heterodinuclear complexes, and to the best of our knowledge, there has been no attempt to adapt this OMO approach to this kind of compounds. The latter approach is that of the natural magnetic orbitals (NMO). These NMOs are defined as the singly occupied molecular orbitals in the monomeric fragments formed by the magnetic centers surrounded by their terminal and bridging ligands. In a few cases, these monomeric fragments actually do exist.[53] Most often, they are defined in a rather arbitrary fashion. This NMO approach can be easily adapted, at least qualitatively, to nonsymmetric homodinuclear as well as heterodinuclear compounds. In Cu(salen)Ni(hfa)$_2$, a way to determine the NMOs would be the following: φ_1 would be the singly occupied molecular orbital for the ground doublet state of an hypothetical Cu(II)B(II) compound of the same symmetry as Cu(salen)Ni(hfa)$_2$, B(II) being a diamagnetic ion replacing Ni(II), for instance Mg(II). As for φ_2 and φ_3, they would be the two singly occupied molecular orbitals for the ground triplet state of an hypothetical A(II)Ni(II) compound, again of the same geometry as the actual Cu(II)Ni(II) compound, A(II) being a diamagnetic ion replacing Cu(II), for instance Ni(II) in square-planar surroundings. Such an approach would be particularly interesting if the Cu(II)B(II) and A(II)Ni(II) compounds did exist. It would be then possible to calculate the local magnetic properties from the φ_μ's and to compare them to the experimental data. In fact, these Cu(II)B(II) and A(II)Ni(II) compounds are not known. Therefore, we have decided to use a somewhat different approach. To determine φ_1, we contracted the nickel atomic orbitals in a way to prevent any orbital interaction between the nickel(II) and its surroundings. In a similar way, to determine φ_2 and φ_3, we contracted the copper atomic orbitals.

All the calculations were performed in the frame of the extended Hückel method. The atomic populations $p_{\mu i}$ in the magnetic orbitals φ_μ, $\mu = 1$–3, are given in Table VI. The atomic spin populations p_i obtained from relations 13 and 14 are given in Table VII and visualized in Figure 6, where the values deduced from the experimental data through multipole analysis are also indi-

Table VI. Atomic Populations $P_{\mu i}$ in the Magnetic Orbitals φ_μ, $\mu = 1$–3 for Cu(salen)Ni(hfa)$_2$

atoms	P_{1i}	P_{2i}	P_{3i}
Cu	0.7436	0.0	0.0
Ni	0.0	0.8493	0.8311
O1	0.0677	0.0199	0.0168
O2	0.0699	0.0009	0.0445
O3	0.0	0.0300	0.0123
O4	0.0	0.0114	0.0210
O5	0.0	0.0042	0.0395
O6	0.0	0.0488	0.0017
N5	0.0603	0.0	0.0
N6	0.0581	0.0	0.0
C11	0.0	0.0	0.0
C21	0.0	0.0	0.0
C1	0.0	0.0090	0.0073
C3	0.0	0.0008	0.0093
C6	0.0	0.0041	0.0155
C8	0.0	0.0221	0.0007

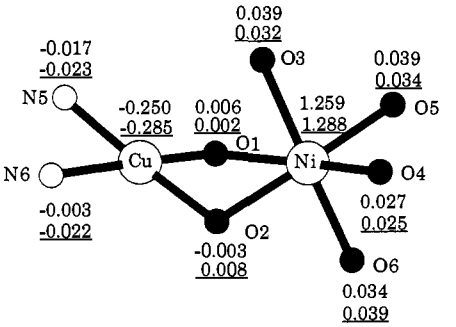

Figure 6. Comparison between atomic spin populations deduced from polarized neutron diffraction through multipole analysis and calculated (underlined figures).

(49) Morgenstern-Badarau, I.; Rerat, M.; Kahn, O.; Jaud, J.; Galy, J. *Inorg. Chem.* **1982**, *21*, 3050.
(50) Lambert, S. L.; Spiro, C. L.; Gagné, R. R.; Hendrickson, D. N. *Inorg. Chem.* **1982**, *21*, 68.
(51) Heine, V. *Group Theory in Quantum Mechanics*; Pergamon Press: Oxford, England, 1960.
(52) Girerd, J. J.; Journaux, Y.; Kahn, O. *Chem. Phys. Lett.* **1981**, *82*, 534.
(53) Kahn, O. *Angew. Chem., Int. Ed. Engl.* **1985**, *24*, 834.

Table VII. Comparison between Atomic Spin Populations Deduced from the PND Experiment, and Calculated from Heitler–London Wave Functions and Extended Hückel Magnetic Orbitals (See Text)

	$S = {}^1/_2$		$S = {}^3/_2$,[a]
	PND	calcd	calcd
Cu	−0.250	−0.285	0.8180
Ni	1.259	1.288	1.8484
O1	0.006	0.0021	0.1148
O2	−0.003	0.008	0.1268
O3	0.039	0.032	0.0465
O4	0.027	0.025	0.0356
O5	0.039	0.034	0.0481
O6	0.034	0.039	0.0556
N5	−0.017	−0.023	0.0663
N6	−0.003	−0.022	0.0639

[a] The hypothetical atomic spin populations in the excited quartet state of Cu(salen)Ni(hfa)$_2$.

cated. From Table VII and Figure 6, one can see that the values calculated in the framework of our semiempirical approach are in fairly good agreement with those deduced from the PND experiment, which suggests that the description of the ground state and the way of determining the magnetic orbitals are satisfying. This facet of our work is discussed further in the next section.

Discussion

This paper reports on the second PND investigation dealing with exchange-coupled dinuclear species. The first one concerned the homodinuclear copper(II) compound $[Cu(H_2O)(bipy)(OH)_2Cu(H_2O)(bipy)](SO_4)\cdot 4H_2O$ with bipy = 2,2′-bipyridine, in which the two copper(II) ions are ferromagnetically coupled.[40] The two main pieces of information arising from the PND study on this copper(II) compound are the following: (i) about 10% of the spin population is located on the bridging oxygen atoms; (ii) significant regions of negative spin density are found on the sides of the bridging atoms, which suggest that the spin polarization plays an important role in the interaction process. Since our study deals with an heterodinuclear system, additional information may be expected, concerning in particular the repartition of the spin density around each of the interacting magnetic centers.

Before discussing our results in a thorough manner, a point needs to be clarified. In our compound, two CuNi units are related through a symmetry center, giving rise to a $[CuNi]_2$ tetranuclear entity with a rather short Cu···Cu separation, 3.432 (1) Å. If the magnetic susceptibility data in the 1.27–300 K temperature range perfectly follow what is expected for an antiferromagnetically coupled CuNi pair with a ground doublet–excited quartet energy gap of 35.4 cm^{-1}, the EPR properties are entirely associated with the bis heterodinuclear entity $[CuNi]_2$. Indeed, the EPR spectrum is that of a triplet state split in zero field and arising from the interaction between the two doublet pair states.[42] However, this interaction between the two symmetry-related CuNi units is extremely weak; it gives rise to a singlet–triplet energy gap inferior to 0.2 cm^{-1}, which is negligible with regard to the applied magnetic field of 5×10^4 G. Therefore, the PND data may be interpreted by considering only the doublet ground state of the Cu(salen)Ni(hfa)$_2$ unit.

The spin density map exhibits a strongly positive zone in the nickel surroundings and a weakly negative zone in the copper surroundings, which is in agreement with the naive representation of the antiferromagnetic coupling between the $S_{Cu} = {}^1/_2$ and $S_{Ni} = 1$ local spins shown:

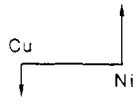

as well as with the expression of the Heitler–London wave function Ψ_+ in (12). Neglecting at first the spin delocalization from the metals toward the bridging and terminal ligands, we expect from (12) a ratio p_{Ni}/p_{Cu} between the spin populations on the metals equal to −4. Actually, the ratio is found equal to −5.04. From our molecular orbital calculation, this slight discrepancy may be attributed to the fact that the magnetic orbital φ_1 centered on copper is more delocalized toward the ligands, in particular the oxygen bridging atoms, than φ_2 and φ_3 centered on nickel.

Let us examine now the spin populations on the oxygen and nitrogen atoms surrounding the metal centers. The most striking finding in this respect is that the spin populations on the bridging atoms O1 and O2 are very weak, and actually within the experimental uncertainties. The first idea coming to mind might be that the interaction between the copper(II) and nickel(II) ions does not occur through the bridging atoms, but rather through the space. Such an idea would be totally erroneous. In fact, the almost negligible spin population on O1 and O2 results from a compensation between positive and negative contributions coming from the nickel(II) and copper(II) ions, respectively. These positive and negative contributions in our calculation appear to be of the order of $\pm 0.025\ \mu_B$. A vivid picture of such a situation would be that of destructive interferences, characterizing the antiferromagnetic nature of the interaction. The almost perfect compensation is also due to the fact that φ_1 is more delocalized toward the atoms O1 and O2 than φ_2 and φ_3, as already mentioned (see Table VI). If the Cu(II)–Ni(II) interaction was ferromagnetic, with a quartet ground state, the interferences on the bridging atoms would be constructive instead of destructive. To illustrate this, we have calculated the hypothetical atomic spin populations for the $S = {}^3/_2$ state of Cu(salen)Ni(hfa)$_2$, from the electronic populations $P_{\mu i}$ of Table VI. The wave function $\Psi_{Ms=3/2}$ for the component $M_S = {}^3/_2$ of the quartet state is

$$\Psi_{Ms=3/2} = |\varphi_1(1)\varphi_2(2)\varphi_3(3)| \tag{15}$$

The spin value $\langle S_i \rangle$ on the atom noted i is then

$$\langle S_i \rangle = {}^1/_2(P_{1i} + P_{2i} + P_{3i}) \tag{16}$$

and the spin population p_i on this atom is given by

$$p_i = g_{3/2}\langle S_i \rangle \tag{17}$$

where $g_{3/2}$ is the Zeeman factor associated with the quartet state and found equal to 2.22.[42] The hypothetical atomic spin populations are tabulated in the third column of Table VII. p_{O1} and p_{O2} on the bridging atoms are found equal to $\sim 0.12\ \mu_B$, which represents quite a significant proportion of the total spin population. Of course, there is no simple and accurate experimental technique for checking these values of the atomic spin populations in the $S = {}^3/_2$ state. The relatively strong spin population found from PND on the bridging atoms of $[Cu(H_2O)(bipy)(OH)_2Cu(H_2O)(bipy)](SO_4)\cdot 4H_2O$[40] is also due to the ferromagnetic nature of the Cu(II)–Cu(II) interaction.

Concerning the spin populations on the peripheral nitrogen and oxygen atoms, there is not much to say. They visualize the delocalization of the magnetic orbitals φ_μ, $\mu = 1$–3. In the $S = {}^1/_2$ ground pair state, the spin populations on the peripheral atoms are on average larger than those on the bridging atoms. In the $S = {}^3/_2$ state, they would be smaller. It is also fair to point out that the extended Hückel calculation was carried out with radially fixed d orbitals, whereas the PND data were analyzed with radially optimized metal multipoles.

In this study, we have looked for an interpretation of the PND data close to the intuition of the chemists working in the field of the exchange-coupled systems. In this respect, it seems to us quite remarkable that simple Heitler–London wave functions constructed by use of the three magnetic orbitals as basis set allow such an interpretation. In our treatment, we did not introduce any additional term as those taken into account in the perturbational calculations of the exchange interaction.[9-16] This confirms the validity, if it was still necessary, of the Heitler–London approach to describing the exchange interaction phenomenon. We must also recognize that a priori the situation was favorable. As a matter of fact, the magnitude of the Cu(II)–Ni(II) interaction in Cu(salen)Ni(hfa)$_2$ is relatively weak, and the energies of the bridging oxygen orbitals are much lower than those of the d metal orbitals. If the bridges were less electronegative, with orbital energies close to those of the metals, the Heitler–London description could be less satisfying.[54]

The method utilized to construct the magnetic orbitals φ_μ likely deserves to be briefly discussed. This method consists of preventing any delocalization of a magnetic orbital toward the metal ion on which it is not centered. This situation is realized by contracting the atomic orbitals of this metal ion. So, the magnetic orbitals strictly describe the unpaired electrons *in the absence* of exchange interaction and the Heitler-London wave functions well correspond to 0th order functions in an approach where the exchange interaction is weak enough to be treated as a perturbation. We think that such a way to define the semilocalized magnetic orbitals could be extended to other problems in molecular magnetism, in particular when dissymmetrical polymetallic entities are involved.

Conclusion

We have emphasized elsewhere[8] that the study of heterodinuclear systems has provided novel and important concepts in the area of molecular magnetism. This specific role of the heterodinuclear compounds is also true as far as the PND technique is concerned. Indeed, the spatial spin distribution is much more informative when the molecular entity is dissymmetrical. In particular, it allows testing of the validity of the wave functions used to describe the ground state. Moreover, owing to the noncompensation of the local spins, the technique is applicable for antiferromagnetically as well as ferromagnetically coupled compounds.

In the case of Cu(salen)Ni(hfa)$_2$ in its doublet ground state, the spatial spin distribution closely follow what the Heitler-London wave functions associated with this state suggest. The ratio p_{Ni}/p_{Cu} of the spin populations on the metals is found equal to -5.04. As for the spin population on the bridges, it is found to be almost negligible. This result in no way indicates that the interaction occurs through space. On the contrary, as expected, the phenolic oxygen atoms play the key role in transmitting the electronic effects; they receive a positive spin density from the nickel(II) and an almost equal (in absolute value) negative spin density from the copper(II).

The PND technique brings new insights on the mechanism of the exchange interaction that no other technique could provide. It deserves to be more often used, particularly in the field of the heteropolymetallic systems. Unfortunately, this technique is still difficult to implement. It requires not only a neutron source but also large and centrosymmetrical single crystals. Nevertheless, we intend to investigate other suitable systems in the near future.

Acknowledgment. We are most grateful to J. Hammann and E. Vincent, who helped us to measure the magnetization curve of Cu(salen)Ni(hfa)$_2$.

Registry No. Cu(salen)Ni(hfa)$_2$, 71073-29-5.

Supplementary Material Available: Tables SVIII-SX giving the atomic coordinates and the parameters used in the extended Hückel calculations (4 pages); table of structure factors (2 pages). Ordering information is given on any current masthead page.

(54) Charlot, M. F.; Kahn, O.; Chaillet, M.; Larrieu, C. *J. Am. Chem. Soc.* **1986**, *108*, 2574.

Radical Cation(s) of (Hexamethyl-) Prismane: Ab Initio Calculations and Nuclear Spin Polarization Results

Krishnan Raghavachari* and Heinz D. Roth*,†

Contribution from AT&T Bell Laboratories, Murray Hill, New Jersey 07974.
Received February 27, 1989

Abstract: Ab initio molecular orbital calculations investigating the nature of the structure and energies of the radical cations of prismane are reported. The effects of polarization functions and electron correlation have been included in these calculations. We also report experimental studies using chemically induced dynamic nuclear polarization that establish the existence of such a radical cation derived from hexamethylprismane. Theoretical studies on the interaction complex between cyclopropenylium cation and cyclopropenyl radical are also reported.

The valence isomers of benzene[1-3] or at least relatively simple derivatives thereof[4-12] are readily available. Their thermal and light-induced rearrangements have been thoroughly explored;[13] some of their thermochemical parameters have been evaluated;[14] and their structural features have been probed by a variety of experimental techniques,[15-21] including microwave spectroscopy as well as electron and X-ray diffraction analysis. In addition, ab initio molecular orbital (MO) calculations have been employed to elucidate a variety of features of these interesting molecules.[14,22,23] On the other hand, the corresponding radical cations have received considerably less attention. We are interested in the radical cations of strained ring systems in general[24] and in those of the four valence isomers of benzene in particular.[25-27] Just as the elucidation of the unique structure of benzene played an important role in the development of organic chemistry,[28] we believe that insight into the structures of the radical cations derived from the (C_6H_6) valence isomers will contribute substantially to

* To whom correspondence should be addressed.
† Current address: Department of Chemistry, Rutgers University, New Brunswick, NJ 08903.

(1) van Tamelen, E. E.; Pappas, S. P. *J. Am. Chem. Soc.* **1963**, *85*, 3297-3298.
(2) Wilzbach, K. E.; Ritscher, J. S.; Kaplan, L. *J. Am. Chem. Soc.* **1967**, *89*, 1031-1032.
(3) Katz, T. J.; Acton, N. *J. Am. Chem. Soc.* **1973**, *95*, 2738-2739.
(4) van Tamelen, E. E.; Pappas, S. P. *J. Am. Chem. Soc.* **1962**, *84*, 3789-3791.
(5) Viehe, H. G.; Merényi, R.; Oth, J. F.; Senders, J. R.; Valange, P. *Angew. Chem., Int. Ed. Engl.* **1964**, *3*, 755-756.
(6) Lemal, D. M.; Staros, J. V.; Austel, V. *J. Am. Chem. Soc.* **1969**, *91*, 3373-3374.
(7) Barlow, G. M.; Haszeldine, R. N.; Hubbard, R. *J. Chem. Soc., Chem. Commun.* **1969**, 202-205.
(8) Graystone, M. W.; Lemal, D. M. *J. Am. Chem. Soc.* **1976**, *98*, 1278-1280.
(9) (a) Weiss, R.; Andrae, S. *Angew. Chem., Int. Ed. Engl.* **1973**, *12*, 150-152, 152-153. (b) Davis, J. H.; Shea, K. J.; Bergman, R. G. *J. Am. Chem. Soc.* **1977**, *99*, 1499-1500. (c) Turro, N. J.; Schuster, G. B.; Bergman, R. G.; Shea, K. J.; Davis, J. H. *J. Am. Chem. Soc.* **1975**, *97*, 4758-4760.

0002-7863/89/1511-7132$01.50/0